PHYSICAL REVIEW D **93,** 054034 (2016)

Insight into $f_0(980)$ through the $B_{(s)}$ charmed decays

Zhi-Qing Zhang,* Si-Yang Wang, and Xing-Ke Ma

Department of Physics, Henan University of Technology, Zhengzhou, Henan 450052, China

(Received 19 January 2016; published 21 March 2016)

Through analyzing the $B_{(s)}$ charmed decays $B^0 \to \bar{D}_0 f_0(980)$ and $B_s \to \bar{D}_0 f_0(980)$ within the framework of the perturbative QCD factorization approach and comparing with the current data, we find that there are two possible regions for the $f_0(980) - f_0(500)$ mixing angle θ: one is centered at 34°–38° and the other falls into 142°–154°. The former can overlap mostly with one of the allowed angle regions extracted from the decay $B^0 \to \bar{D}_0 f_0(500)$. The branching fractions of B_s decay modes are less sensitive to the mixing angle compared with those of B decay modes. Especially, for the decay $B_s \to D^0 f_0(980)$, its branching fraction changes only slightly between $(1.2\text{–}1.8) \times 10^{-7}$ when the mixing angle θ runs from 0° to 180°. All of our results support the picture that the $f_0(980)$ is dominated by the two-quark component in the B decay dynamic mechanism. Furthermore, the $s\bar{s}$ component is more important than the $q\bar{q} = (u\bar{u} + d\bar{d})/\sqrt{2}$ component. This point is different from $f_0(500)/\sigma$. Last but not least, our picture is not in conflict with the popular four-quark explanation.

DOI: 10.1103/PhysRevD.93.054034

I. INTRODUCTION

Up to now the quark-level substructure of scalar mesons is still not well understood. Especially, the slight scalar mesons, including $f_0(500)(\sigma)$, $f_0(980)$, $K_0^*(800)(\kappa)$, and $a_0(980)$, which form a SU(3) flavor nonet, are considered as either two-quark states or tetraquark states (diquark and anti-diquark structure) as originally advocated by Jaffe [1]. Certainly, there are other different SU(3) scenarios about scalar mesons [2]. If one considers these light scalar mesons as two-quark states, $q\bar{q}$ structure, there are experiments which indicate that the heaviest one $f_0(980)$ and the lightest one $f_0(500)$ in this SU(3) nonet must have a mixing

$$\begin{aligned} |f_0(980)\rangle &= |s\bar{s}\rangle \cos\theta + |n\bar{n}\rangle \sin\theta, \\ |f_0(500)\rangle &= -|s\bar{s}\rangle \sin\theta + |n\bar{n}\rangle \cos\theta, \end{aligned} \tag{1}$$

where $|n\bar{n}\rangle \equiv (u\bar{u} + d\bar{d})/\sqrt{2}$. For the mixing angle θ, there are several different values from experimental measurements. A mixing angle $\theta = 34° \pm 6°$ was determined from the decays $J/\Psi \to f_0\phi, f_0\omega$, and $31° \pm 5°$ or $42° \pm 7°$ from the decays $D_{(s)} \to f_0(980)\pi$, $f_0(980)K$, while a range $35° < |\theta| < 55°$ was given from the analysis of three body decay $D_s^+ \to \pi^+\pi^+\pi^-$. An analysis of $f_0(980) - f_0(500)$ mixing by using the light cone QCD sum rules [3] yielded $\theta = 27° \pm 13°$ and $\theta = 41° \pm 11°$. The value of $\theta \sim 34°$ or $\sim 146°$ was obtained in the decays $B_s \to J/\psi f_0(980)$, $J/\psi\sigma$ [4]. Ochs [5] found $\theta = 30° \pm 3°$ by averaging over several decay processes. The authors of Ref. [6] provided a limit on the mixing angle $\theta < 29°$ at 90% confidence. As we know, the mixing between $f_0(980) - \sigma$ is something like that in $\eta - \eta'$, but with many more uncertainties. In order to explain the $K - \eta'$ puzzle, some complex mixing mechanisms including gluon even η_c meson in $\eta - \eta'$ were also considered [7–9]. This led people to conjecture that $f_0(980)$ and $f_0(500)$ may not be simple quark-antiquark states, and perhaps there exists a more complicated structure except the $f_0(980) - \sigma$ mixing.

Recently, the decays $B_{(s)} \to \bar{D} f_0(500)$, $\bar{D} f_0(980)$ were measured by the LHCb Collaboration [10,11],

$$\begin{aligned} &\mathcal{B}(B^0 \to \bar{D}^0 f_0(500)) \\ &\quad = (11.2 \pm 0.8 \pm 0.5 \pm 2.1 \pm 0.5) \times 10^{-5}, \end{aligned} \tag{2}$$

$$\begin{aligned} &\mathcal{B}(B^0 \to \bar{D}^0 f_0(980)) \\ &\quad = (1.34 \pm 0.25 \pm 0.10 \pm 0.46 \pm 0.06) \times 10^{-5}, \end{aligned} \tag{3}$$

$$\begin{aligned} &\mathcal{B}(B_s^0 \to \bar{D}^0 f_0(980)) \\ &\quad = (1.7 \pm 1.0 \pm 0.5 \pm 0.1) \times 10^{-6}, \end{aligned} \tag{4}$$

where the first and the second uncertainties are statistical and experimental systematic errors, respectively, and the third uncertainties are from the model-dependent error. The fourth uncertainties in Eq. (2) and Eq. (3) are from the normalization $B^0 \to D^*(2010)^-\pi^+$ channel. We see there exist larger statistical errors in the B_s^0 decay and the model-dependent error in the first two B^0 decays. By using these new data, we will try to constrain the mixing angle between $f_0(980)$ and σ through these $B_{(s)}$ decays in the perturbative QCD (pQCD) approach. There was a work about constraining the mixing angle through $B_s^0 \to J/\Psi f_0(980)$, $J/\Psi\sigma$ decays [4], but two different approaches were used in the same decay channel: the factorizable contribution

*zhangzhiqing@haut.edu.cn

and vertex corrections are calculated in the QCD factorization (QCDF) approach, while the hard spectator scattering corrections are calculated in the pQCD approach. So one may suspect its rationality and reliability in determining the mixing angle between $f_0(980)-\sigma$. The B meson decays with a D meson involved in the final states have been studied in the pQCD approach, such as $B\to DP, DV, DA$ [12–15], where P, V, A represent pseudoscalar, vector, and axial-vector mesons, respectively. Most of the predictions can well explain the experimental data. While an explicit calculation for the branching ratio of the decay $B_s^0\to\bar{D}^0 f_0(980)$ gives $(3.5^{+1.26+0.56}_{-1.15-0.77})\times 10^{-5}$ [16], this is quite different from the present experimental result. So we would like to systematically study the decays $B_{(s)}\to\bar{D}f(980)$ in the pQCD approach, including the Cabibbo-Kobayashi-Maskawa (CKM) suppressed decays $B_{(s)}\to Df_0(980)$. At last, the decays $B_{(s)}\to\bar{D}^* f(980)$, $D^* f_0(980)$ are also considered.

The layout of this paper is as follows. In Sec. II, decay constants and light-cone distribution amplitudes of the relevant mesons are introduced. In Sec. III, we then analyze these decay channels using the pQCD approach. The numerical results and the discussions are given in Sec. IV. Conclusions are presented in the final part.

II. DECAY CONSTANTS AND DISTRIBUTION AMPLITUDES

For the wave function of the heavy $B_{(s)}$ meson, we take

$$\Phi_{B_{(s)}}(x,b)=\frac{1}{\sqrt{2N_c}}(\not{P}_{B_{(s)}}+m_{B_{(s)}})\gamma_5\phi_{B_{(s)}}(x,b). \quad (5)$$

Here only the contribution of the first Lorentz structure $\phi_{B_{(s)}}(x,b)$ is taken into account, since the contribution of the second Lorentz structure $\bar{\phi}_{B_{(s)}}$ is numerically small [17] and can be neglected. For the distribution amplitude $\phi_{B_{(s)}}(x,b)$ in Eq. (5), we adopt the following model:

$$\phi_{B_{(s)}}(x,b)=N_{B_{(s)}}x^2(1-x)^2\exp\left[-\frac{M_{B_{(s)}}^2x^2}{2\omega_b^2}-\frac{1}{2}(\omega_b b)^2\right], \quad (6)$$

where ω_b is a free parameter and is taken to be $\omega_b=0.4\pm0.04(0.5\pm0.05)$ GeV for $B(B_s)$ in numerical calculations, and $N_B=101.445$ ($N_{B_s}=63.671$) is the normalization factor for $\omega_b=0.4$ (0.5). For the B_s meson, the SU(3) breaking effects are taken into consideration.

As for the wave functions of the D meson, we use the form derived in Ref. [18],

$$\int\frac{d^4\omega}{(2\pi)^4}e^{ik\cdot\omega}\langle 0|\bar{c}_\beta(0)u_\gamma(\omega)|\bar{D}^0\rangle = -\frac{i}{\sqrt{2N_c}}[(\not{P}_D+m_D)\gamma_5]_{\gamma\beta}\phi_D(x,b), \quad (7)$$

$$\int\frac{d^4\omega}{(2\pi)^4}e^{ik\cdot\omega}\langle 0|\bar{c}_\beta(0)u_\gamma(\omega)|\bar{D}^{*0}\rangle = -\frac{i}{\sqrt{2N_c}}[(\not{P}_{D^*}+m_{D^*})\not{\epsilon}_L]_{\gamma\beta}\phi_{D^*}^L(x,b), \quad (8)$$

where ϵ_L is the longitudinal polarization vector. In this work only the longitudinal polarization component is used. Here we take the best-fitted form $\phi_D^{(*)}$ from B to charmed meson decays derived in [12] as

$$\phi_D(x,b)=\frac{f_D}{2\sqrt{2N_c}}6x(1-x)[1+C_D(1-2x)]\exp\left[\frac{-\omega^2b^2}{2}\right]. \quad (9)$$

For the wave function $\phi_{D_s}(x,b)$, it has the similar expression as $\phi_D(x,b)$ except with different parameters and is given as follows: $f_D=204.6$ MeV, $f_{D_s}=257.5$ MeV, and $C_{D_{(s)}}=0.5$ (0.4), $\omega_{D_{(s)}}=0.1$ (0.2) [19]. For the wave function $\phi_{D_{(s)}^*}(x,b)$, we take the same distribution amplitude with that of the pseudoscalar meson $D_{(s)}$ because of their small mass difference, except with different decay constants $f_{D^*}=270$ MeV and $f_{D_s^*}=310$ MeV [20].

Since the neutral scalar meson $f_0(980)$ cannot be produced via the vector current, we have $\langle f_0(p)|\bar{q}_2\gamma_\mu q_1|0\rangle=0$ [the abbreviation f_0 denotes the $f_0(980)$ for simplicity]. Taking the $f_0(980)-\sigma$ mixing into account, the scalar current $\langle f_0(p)|\bar{q}_2q_1|0\rangle=m_S\bar{f}_S$ can be written as

$$\langle f_0^n|d\bar{d}|0\rangle=\langle f_0^n|u\bar{u}|0\rangle=\frac{1}{\sqrt{2}}m_{f_0}\tilde{f}_{f_0}^n,$$
$$\langle f_0^s|s\bar{s}|0\rangle=m_{f_0}\tilde{f}_{f_0}^s, \quad (10)$$

where $f_0^{(n,s)}$ represent the quark flavor states for the $n\bar{n}$ and $s\bar{s}$ components of the f_0 meson, respectively. As the scalar decay constants $\tilde{f}_{f_0}^n$ and $\tilde{f}_{f_0}^s$ are very close [21], we can assume $\tilde{f}_{f_0}^n=\tilde{f}_{f_0}^s$ and denote them as $\bar{f}_{f_0}$ in the following.

The twist-2 and twist-3 light-cone distribution amplitudes (LCDAs) for the different components of $f_0(980)$ are defined by

$$\langle f_0(p)|\bar{q}(z)_l q(0)_j|0\rangle = \frac{1}{\sqrt{2N_c}}\int_0^1 dx e^{ixp\cdot z}\{\not{p}\Phi_{f_0}(x)+m_{f_0}\Phi_{f_0}^S(x) + m_{f_0}(\not{n}_+\not{n}_- -1)\Phi_{f_0}^T(x)\}_{jl}, \quad (11)$$

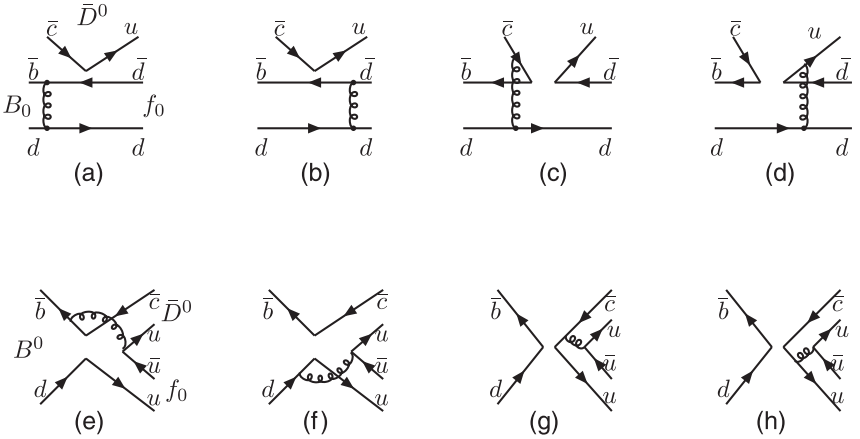

FIG. 1. Diagrams contributing to the $B^0 \to \bar{D}^0 f_0(980)$ decay.

where we assume $f_0^n(p)$ and $f_0^s(p)$ are the same and denote them as $f_0(p)$, and n_+ and n_- are lightlike vectors: $n_+ = (1, 0, 0_T)$, $n_- = (0, 1, 0_T)$. The normalization of the distribution amplitudes are related to the decay constants,

$$\int_0^1 dx \Phi_{f_0}(x) = \int_0^1 dx \Phi_{f_0}^T(x) = 0,$$
$$\int_0^1 dx \Phi_{f_0}^S(x) = \frac{\bar{f}_{f_0}}{2\sqrt{2N_c}}. \tag{12}$$

The twist-2 LCDA $\Phi_{f_0}(x)$ can be expanded in terms of Gegenbauer polynomials as

$$\Phi_{f_0}(x) = \frac{1}{2\sqrt{2N_c}} \bar{f}_{f_0} 6x(1-x)\left[B_0 + \sum_{m=1} B_m C_n^{3/2}(2x-1)\right], \tag{13}$$

with the decay constant $\bar{f}_{f_0} = 0.18 \pm 0.015$ GeV [22]. It is noticed that all the even Gegenbauer momentums vanish due to the charge conjugation invariance. As for the odd Genbauer momentums, only the first term is kept and the value of the coefficient is taken as $B_1 = -0.78 \pm 0.08$ [21]. For the twist-3 LCDA, we also take the first term of the Gegenbauer expansion, i.e. the asymptotic form,

$$\Phi_{f_0}^S(x) = \frac{1}{2\sqrt{2N_c}} \bar{f}_{f_0}, \qquad \Phi_{f_0}^T(x) = \frac{1}{2\sqrt{2N_c}} \bar{f}_{f_0}(1-2x). \tag{14}$$

III. THE PERTURBATIVE QCD CALCULATION

The weak effective Hamiltonian $H_{\rm eff}$ for the charmed $B_{(s)}$ decays $B_{(s)} \to \bar{D} f_0(980)$, $\bar{D}^* f_0(980)$, is composed only by the tree operators and given by

$$H_{\rm eff} = \frac{G_F}{\sqrt{2}} V_{cb}^* V_{uq} [C_1(\mu) O_1(\mu) + C_2(\mu) O_2(\mu)], \tag{15}$$

where the tree operators are written as

$$O_1 = (\bar{c}_\alpha b_\beta)_{V-A} (\bar{D}_\beta u_\alpha)_{V-A},$$
$$O_2 = (\bar{c}_\alpha b_\alpha)_{V-A} (\bar{D}_\beta u_\alpha)_{V-A}, \tag{16}$$

where D represents $d(s)$. These decays with larger CKM matrix elements (say the $\bar{b} \to \bar{d}$ transition, $|V_{cb} V_{ud}| = 0.04$) are called CKM allowed decays. Another kind of decays $B_{(s)} \to D^0 f_0$, $D^{*0} f_0$, $D_{(s)}^+ f_0$, $D_{(s)}^{*+} f_0$ with smaller CKM matrix elements (in the case of $b \to d$ transition, $|V_{ub} V_{cd}| = 0.00093$) are called CKM suppressed decays, and the corresponding weak effective Hamiltonian is given as

$$H_{\rm eff} = \frac{G_F}{\sqrt{2}} V_{ub}^* V_{cq} [C_1(\mu) O_1(\mu) + C_2(\mu) O_2(\mu)]. \tag{17}$$

Here we take the decay $B^0 \to \bar{D}^0 f_0$ as an example, whose leading-order Feynman diagrams are shown in Fig. 1. The Feynman diagrams in the first row are for the emission types, where Figs. 1(a) and 1(b) are the factorizable diagrams, Figs. 1(c) and 1(d) are the nonfactorizable ones, and their amplitudes are written as

$$\mathcal{F}_{B\to f_0}^{\bar{D}} = 8\pi C_F M_B^4 f_D \int_0^1 dx_1 dx_2 \int_0^\infty b_1 db_1 b_2 db_2 \phi_B(x_1, b_1)[(1+x_2)\phi_{f_0}(x_2) + r_f(1-2x_2)(\phi_{f_0}^s(x_2) + \phi_{f_0}^t(x_2))]$$
$$\times E_e(t_a) h_e(x_1, x_2(1-r_D^2), b_1, b_2) S_t(x_2) + 2r_f \phi_{f_s}(x_2) E_e(t_b) h_e(x_2, x_1(1-r_D^2), b_2, b_1) S_t(x_1)], \tag{18}$$

$$\mathcal{M}^{\bar{D}}_{B\to f_0} = 32\pi C_f m_B^4/\sqrt{2N_C}\int_0^1 dx_1dx_2dx_3\int_0^\infty b_1db_1b_3db_3\phi_B(x_1,b_1)\phi_D(x_3,b_3)$$
$$\times\{[(x_3-1)\phi_{f_0}(x_2)+r_{f_0}x_2(\phi^s_{f_0}(x_2)-\phi^t_{f_0}(x_2))-4r_{f_0}r_cr_D\phi^s_{f_0}(x_2)]$$
$$\times E_{en}(t_c)h^c_{en}(x_1,x_2(1-r_D^2),x_3,b_1,b_3)+E_{en}(t_d)h^d_{en}(x_1,x_2(1-r_D^2),x_3,b_1,b_3)$$
$$\times[(x_2+x_3)\phi_{f_0}(x_2)-r_{f_0}x_2(\phi^s_{f_0}(x_2)+\phi^t_{f_0}(x_2))]\}, \tag{19}$$

with the mass ratios $r_{f_0}=m_{f_0}/M_B$, $r_D=m_D/M_B$, and $r_c=m_c/M_B$. The evolution factors evolving the scale t and the hard functions of the hard part of factorization amplitudes are listed as

$$E_e(t)=\alpha_s(t)\exp[-S_B(t)-S_{f_0}(t)], \tag{20}$$

$$E_{en}(t)=\alpha_s(t)\exp[-S_B(t)-S_{f_0}(t)-S_D(t)|_{b_1=b_2}], \tag{21}$$

$$h_e(x_1,x_2,b_1,b_2)$$
$$=K_0(\sqrt{x_1x_2}m_Bb_1)[\theta(b_1-b_2)K_0(\sqrt{x_2}m_Bb_1)I_0(\sqrt{x_2m_Bb_2}) \quad +\theta(b_2-b_1)K_0(\sqrt{x_2m_Bb_2})I_0(\sqrt{x_2m_Bb_1})], \tag{22}$$

$$h^j_{en}(x_1,x_2,x_3,b_1,b_3)=[\theta(b_1-b_3)K_0\Big(\sqrt{x_1x_2(1-r_D^2)}m_Bb_1\Big)I_0\Big(\sqrt{x_1x_2(1-r_D^2)}m_Bb_3\Big)$$
$$+(b_1\leftrightarrow b_3)]\begin{pmatrix}K_0(A_jm_Bb_3) & \text{for } A_j^2\geq 0\\ \frac{i\pi}{2}H_0^{(1)}\Big(\sqrt{|A_j^2|}m_Bb_3\Big) & \text{for } A_j^2\leq 0\end{pmatrix}, \tag{23}$$

with the variables $A_j^2(j=c,d)$ listed as

$$A_c^2=r_c^2-(1-x_1-x_3)(x_2(1-r_D^2)+r_D^2), \tag{24}$$

$$A_d^2=(x_1-x_3)x_2(1-r_D^2). \tag{25}$$

The hard scale t and the expression of the Sudakov factor in each amplitude can be found in the Appendix. As we know, the double logarithms $\alpha_s\ln^2x$ produced by the radiative corrections are not small expansion parameters when the end-point region is important. In order to improve the perturbative expansion, threshold resummation of these logarithms to all order is needed, which leads to a quark jet function

$$S_t(x)=\frac{2^{1+2c}\Gamma(3/2+c)}{\sqrt{\pi}\Gamma(1+c)}[x(1-x)]^c, \tag{26}$$

with $c=0.32$. It is effective to smear the end-point singularity with a momentum fraction $x\to 0$. This factor will also appear in the factorizable annihilation type amplitudes.

The amplitudes for the Feynman diagrams in the second row can be obtained by the Feynman rules and are given as

$$\mathcal{M}^{\bar{D}}_{ann}=32\pi C_fm_B^4/\sqrt{2N_C}\int_0^1 dx_1dx_2dx_3\int_0^\infty b_1db_1b_3db_3\phi_B(x_1,b_1)\phi_D(x_3,b_3)\{E_{an}(t_e)h^e_{an}(x_1,x_2,x_3,b_1,b_3)[x_3\phi_{f_0}(x_2)$$
$$+r_Dr_{f_0}((x_2-x_3-3)\phi^s_{f_0}(x_2)+(x_2+x_3-1)\phi^t_{f_0}(x_2))]+E_{an}(t_f)h^f_{an}(x_1,x_2,x_3,b_1,b_3)[(x_2-1)\phi_{f_0}(x_2)$$
$$+r_Dr_{f_0}((1+x_3-x_2)\phi^s_{f_0}(x_2)+(x_2+x_3-1)\phi^t_{f_0}(x_2))]\}, \tag{27}$$

$$\mathcal{F}^{\bar{D}}_{ann}=-8\pi C_ff_Bm_B^4\int_0^1 dx_2dx_3\int_0^\infty b_2db_2b_3db_3\phi_D(x_3,b_3)\{[(1-x_2)\phi_{f_0}(x_2)-2r_{f_0}r_D$$
$$\times x_2\phi^t_{f_0}(x_2)+2r_Dr_{f_0}(x_2-2)\phi^s_{f_0}(x_2)]E_{af}(t_g)h_{af}(x_3,(1-x_2)(1-r_D^2),b_3,b_2)$$
$$+E_{af}(t_h)h_{af}(x_2,x_3(1-r_D^2),b_2,b_3)[-x_3\phi_{f_0}(x_2)+2r_Dr_{f_0}(x_3+1)\phi^s_{f_0}(x_2)]\}. \tag{28}$$

Similarly, $F^{\bar{D}}_{ann}(M^{\bar{D}}_{ann})$ are the (non)factorizable annihilation type amplitudes, where the evolution factors E evolving the scale t and the hard functions of the hard part of factorization amplitudes are listed as

$$E_{an}(t) = \alpha_s(t)\exp[-S_B(t) - S_D(t) - S_{f_0}(t)|_{b_2=b_3}], \tag{29}$$

$$E_{af}(t) = \alpha_s(t)\exp[-S_D(t) - S_{f_0}(t)], \tag{30}$$

$$h^j_{an}(x_1,x_2,x_3,b_1,b_3) = i\frac{\pi}{2}[\theta(b_1-b_3)H_0^{(1)}\left(\sqrt{x_2x_3(1-r_D^2)}m_Bb_1\right)J_0\left(\sqrt{x_2x_3(1-r_D^2)}m_Bb_3\right) + (b_1 \leftrightarrow b_3)]\begin{pmatrix} K_0(L_jm_Bb_1) & \text{for } L_j^2 \geq 0 \\ \frac{i\pi}{2}H_0^{(1)}\left(\sqrt{|L_j^2|}m_Bb_1\right) & \text{for } L_j^2 \leq 0 \end{pmatrix}, \tag{31}$$

$$h_{af}(x_2,x_3,b_2,b_3) = \left(i\frac{\pi}{2}\right)^2 H_0^{(1)}(\sqrt{x_2x_3}m_Bb_2)[\theta(b_2-b_3)H_0^{(1)}(\sqrt{x_3}m_Bb_2)J_0(\sqrt{x_3}m_Bb_3) + (b_2 \leftrightarrow b_3)], \tag{32}$$

where the definitions of $L_j^2(j = e, f)$ are written as

$$L_e^2 = r_b^2 - (1-x_3)(1-(1-x_2)(1-r_D^2) - x_1), \tag{33}$$

$$L_f^2 = x_3(x_1 - (1-x_2)(1-r_D^2)). \tag{34}$$

The functions $H_0^{(1)}$, J_0, K_0, I_0, which appear in the upper hard kernel h_e, h^j_{en}, h^j_{an}, h_{af}, are the (modified) Bessel functions, which are obtained from the Fourier transformations of the quark and gluon propagators. Combining the above amplitudes, one can easily write down the total decay amplitudes of each considered channel,

$$\mathcal{A}(B^0 \to \bar{D}^0 f_0(980)) = \frac{G_F}{\sqrt{2}}V_{cb}^*V_{ud}(F^{\bar{D}}_{B\to f_0}a_2 + M^{\bar{D}}_{B\to f_0}C_2 + M^{\bar{D}}_{ann}C_2 + F^{\bar{D}}_{ann}a_2), \tag{35}$$

$$\mathcal{A}(B^0 \to D^0 f_0(980)) = \frac{G_F}{\sqrt{2}}V_{ub}^*V_{cd}(F^{D}_{B\to f_0}a_2 + M^{D}_{B\to f_0}C_2 + M^{f_0}_{ann}C_2 + F^{f_0}_{ann}a_2), \tag{36}$$

$$\mathcal{A}(B_s^0 \to \bar{D}^0 f_0(980)) = \frac{G_F}{\sqrt{2}}V_{cb}^*V_{us}(F^{D}_{B\to f_0}a_2 + M^{D}_{B\to f_0}C_2 + M^{D}_{ann}C_2 + F^{D}_{ann}a_2), \tag{37}$$

$$A(B_s^0 \to D^0 f_0(980)) = \frac{G_F}{\sqrt{2}}V_{ub}^*V_{cs}(F^{D}_{B\to f_0}a_2 + M^{D}_{B\to f_0}C_2 + M^{f_0}_{ann}C_2 + F^{f_0}_{ann}a_2), \tag{38}$$

$$\mathcal{A}(B^+ \to D^+ f_0(980)) = \frac{G_F}{\sqrt{2}}V_{ub}^*V_{cd}(F^{D}_{B\to f_0}a_1 + M^{D}_{B\to f_0}C_2/3 + M^{f_0}_{ann}C_2/3 + F^{f_0}_{ann}a_1), \tag{39}$$

$$\mathcal{A}(B^+ \to D_s^+ f_0(980)) = \frac{G_F}{\sqrt{2}}V_{ub}^*V_{cs}(F^{D}_{B\to f_0}a_1 + M^{D}_{B\to f_0}C_2/3 + M^{f_0}_{ann}C_2/3 + F^{f_0}_{ann}a_1), \tag{40}$$

and likewise for the corresponding decays with the pseudoscalar meson D replaced by the vector meson D^*.

IV. NUMERICAL RESULTS AND DISCUSSIONS FOR $B_{(s)}$ DECAYS

We use the following input parameters for numerical calculations [19]:

$$f_B = 190\ \text{MeV}, \quad f_{B_s} = 230\ \text{MeV}, \quad M_B = 5.28\ \text{GeV}, \quad M_{B_s} = 5.37\ \text{GeV}, \tag{41}$$

$$\tau_B^{\pm} = 1.638\times10^{-12}\ \text{s}, \quad \tau_{B^0} = 1.519\times10^{-12}\ \text{s}, \quad \tau_{B_s} = 1.512\times10^{-12}\ \text{s}, \tag{42}$$

$$M_{D^0} = 1.869\ \text{GeV}, \quad M_{D_s^+} = 1.968\ \text{GeV}, \quad M_{D^{*0}} = 2.007\ \text{GeV}, \quad M_{D_s^{*+}} = 2.112\ \text{GeV}. \tag{43}$$

For the CKM matrix elements, we adopt the Wolfenstein parametrization and the updated values $A = 0.814$, $\lambda = 0.22537$, $\bar{\rho} = 0.117 \pm 0.021$, and $\bar{\eta} = 0.353 \pm 0.013$ [19].

In the $B_{(s)}$-rest frame, the decay rates of $B_{(s)} \to D^{(*)}_{(s)}f_0(980)$ can be written as

$$\mathcal{BR}(B_{(s)} \to D^{(*)}_{(s)}f_0(980)) = \frac{\tau_{B_{(s)}}}{16\pi M_B}(1 - r^2_{D^{(*)}_{(s)}})\mathcal{A}, \tag{44}$$

where $\mathcal{A}$ is the total decay amplitude of each considered decay, which has been given in the last section.

Using the input parameters and the wave functions as specified in this section and Sec. II, we give the dependencies of the branching ratios $\mathcal{BR}(B^0 \to \bar{D}^0 f_0(980))$ and $\mathcal{BR}(B_s \to \bar{D}^0 f_0(980))$ on the mixing angle θ shown in Fig. 2. Combining these two panels, one can find that the allowed mixing angle lies in the range $135° < \theta < 158°$ at the large angle region. It is not strange that, as mentioned before, the large mixing angle $\theta \sim 146°$ is also obtained in the analysis of $B_s \to J/\psi f_0(980)$, $J/\psi\sigma$ decays [4]. In the

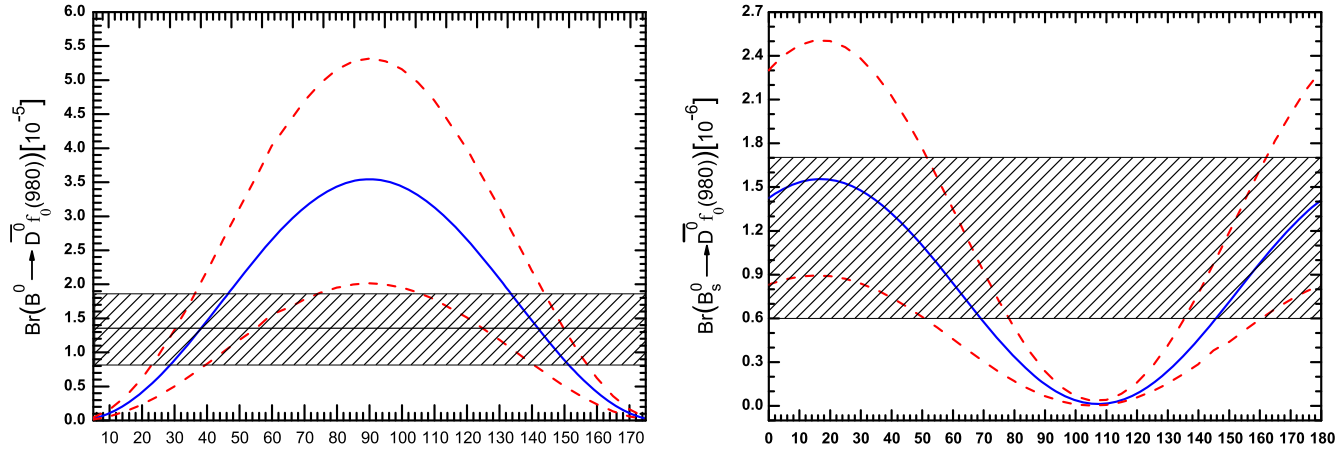

FIG. 2. Dependencies of the branching ratios $\mathcal{BR}(B^0 \to \bar{D}^0 f_0(980))$ (left) and $\mathcal{BR}(B_s \to \bar{D}^0 f_0(980))$ (right) on the mixing angle θ. In each panel, the solid (blue) curve represents the central value of the theoretical prediction, and the two dashed (red) curves correspond to the upper and lower limits. On the left panel, the shaded band shows the allowed region and the horizontal bisector the central value of $\mathcal{BR}(B^0 \to \bar{D}^0 f_0(980)) = (1.34 \pm 0.54) \times 10^{-5}$ for data. On the right panel, for the large uncertainties with the branching ratio, only the half-width band is given; that is to say, the upper edge line represents the center value of data $\mathcal{BR}(B_s \to \bar{D}^0 f_0(980)) = (1.7 \pm 1.1) \times 10^{-6}$, and the lower edge line represents the experimental lower limit.

following we mainly discuss the region with the mixing angle less than 90°. For the branching ratio of the decay $B^0 \to \bar{D}^0 f_0(980)$, the experimental value $(1.34 \pm 0.54) \times 10^{-5}$ with 2.5σ can give a stronger constrain on the mixing angle, and in the range of $29° < \theta < 46°$, the central theoretical values agree well with the data. But if the theoretical uncertainties are included, the range will become wider. Although the branching ratio $\mathrm{Br}(B_s \to \bar{D}^0 f_0(980))$ with large uncertainty cannot give stringent constrain on the value of the mixing angle, we can get some hints from the data: If we take the mixing angle $\theta = 0°$, that is, we consider that the scalar meson $f_0(980)$ is composed entirely of the two-quark component $s\bar{s}$, the corresponding branching ratio is about 1.4×10^{-6}, which is a little lower than the experimental value. If we consider the small mixing with $q\bar{q} = (u\bar{u} + q\bar{q})/\sqrt{2}$, the branching ratio will get an enhancement for the interference between the two different kinds of amplitudes from the different quark components, the maximal value for the branching ratio can be obtained at the mixing angle $\theta = 19°$, and it arrives at 1.56×10^{-6} (shown in the right panel of Fig. 2). But if we take such a small mixing angle, say about 20°, it will make the branching ratio of the decay $B^0 \to \bar{D}^0 f_0(980)$ undershoot the shaded band in the left panel of Fig. 2, which represents the experimental allowed region. The mixing angle θ between $f_0(980)$ and $f_0(500)$ should not be too large, say larger than 70°. If so, the predicted branching ratios of both the decays $B_s \to \bar{D}^0 f_0(980)$ and $B^0 \to \bar{D}^0 f_0(980)$ will deviate from the data even with the large errors taken into account. So we get the conclusion that the two-quark component should be dominant for B meson decays in the dynamic mechanism. Furthermore, the $s\bar{s}$ component is more important than the $q\bar{q}$ component. But it is not in conflict with the dominant four-quark structure in explaining the mass degeneracy of $f_0(980)$ and $a_0(980)$, and the narrower decay width of $f_0(980)$ than that of $f_0(500)$. In the following, we will discuss the mixing angle by considering the ratio of branching fractions. There are some advantages in considering the ratio, because one can eliminate the systematic errors on the experimental side and avoid the hadronic uncertainties, such as the decay constants and the Gegenbauer moments of the final states on the theoretical side. From the data, one can find that the ratio of these two branching fractions $\mathcal{BR}(B^0 \to \bar{D}^0 f_0(980))/\mathcal{BR}(B_s \to \bar{D}^0 f_0(980)) = 7.88 \pm 5.60$. Unfortunately, here the uncertainty is mainly from the statistical error in the decay $B_s \to \bar{D}^0 f_0(980)$, so the errors of the ratio are not much improved compared to those of the branching ratio of each decay mode. Certainly, here we consider a simple method; maybe there is a much better approach for the experimentalists to greatly reduce the errors from this ratio. So we advise the reader to accurately measure this ratio in an experiment, because it is important to further restrict the mixing angle θ between $f_0(980)$ and $f_0(500)(\sigma)$. The ratio can change in a very large range with the mixing angle taking different values; especially for $\theta = 90°$, the branching ratio of $B_s \to \bar{D}^0 f_0(980)$ is very small and will be exactly equal to zero if the contribution from $q\bar{q} = (u\bar{u} + d\bar{d})/\sqrt{2}$ is turned off, while $\mathcal{BR}(B^0 \to \bar{D}^0 f_0(980))$ arrives at its maximal value. Then it will be meaningless for the ratio, not mentioning the errors. For the sake of comparison, we give two regions for the mixing angle shown in Fig. 3. If combining these four panels in Fig. 2 and Fig. 3 together, one will get two further shrunken mixing angle ranges $22° < \theta < 58°$ and $141° < \theta < 158°$. In view of the present large uncertainties from data and theory, it will be difficult to

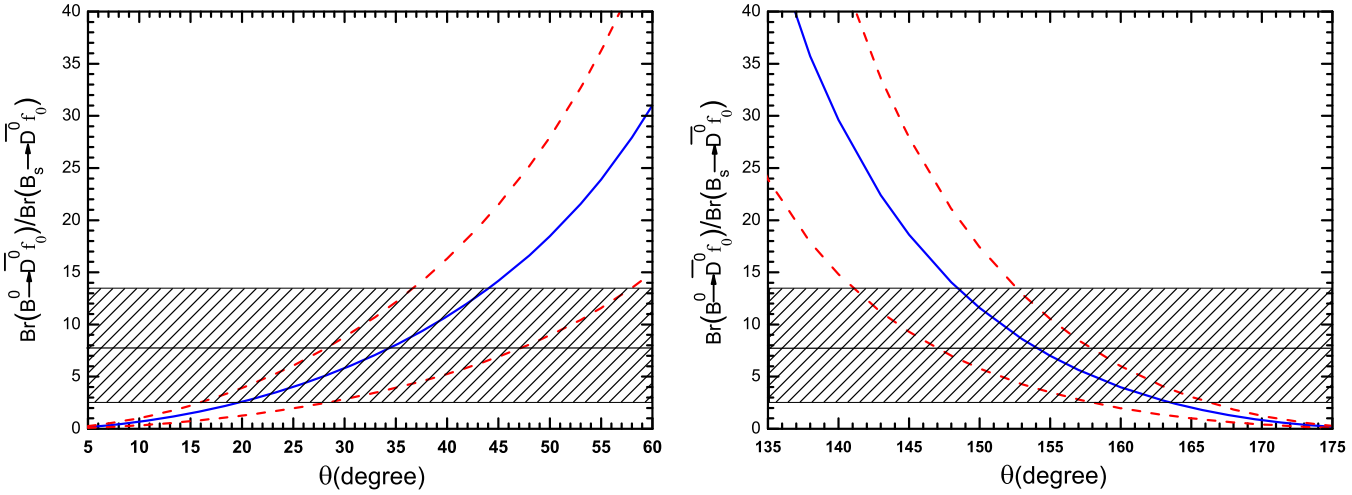

FIG. 3. Dependencies of the ratio between $\mathcal{BR}(B^0 \to \bar{D}^0 f_0(980))$ and $\mathcal{BR}(B_s \to \bar{D}^0 f_0(980))$ on the mixing angle θ at different regions. The shaded band shows the allowed region and the horizontal bisector of the central value of $\mathcal{BR}(B^0 \to \bar{D}^0 f_0(980))/\mathcal{BR}(B_s \to \bar{D}^0 f_0(980)) = 7.88 \pm 5.60$ for data.

get a unitary value for the mixing angle. But even if more precise data are available, we still cannot get the unitary value. This argument might be reasonable that there must be some influence from other components in $f_0(980)$, such as gluon, four quark component, and $K\bar{K}$ threshold effect, which we cannot handle at present. Nevertheless, one cannot deny that the two-quark component in $f_0(980)$ is dominant in the B decay dynamic mechanism, and the $s\bar{s}$ component is more important than the $q\bar{q}$ component.

Up to now we still do not analyze the decay $B^0 \to \bar{D}^0\sigma$, although the data of this channel is available. There are many uncertainties from the decay constant and the LCDAs

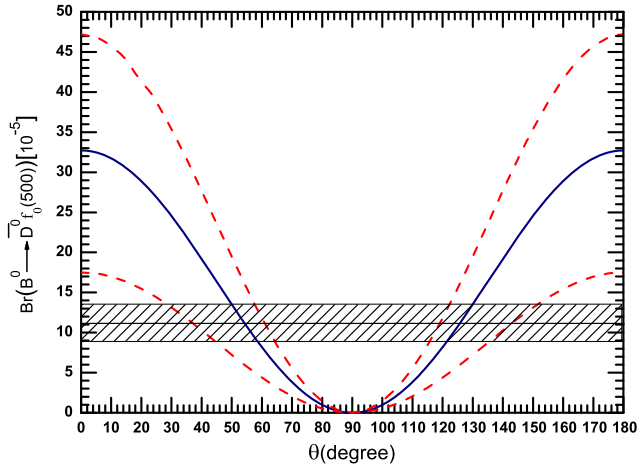

FIG. 4. Dependence of the branching ratio $\mathcal{BR}(B^0 \to \bar{D}^0 f_0(500))$ on the mixing angle θ. The solid (blue) curve represents the central value of the theoretical prediction, and the two dashed (red) curves correspond to the upper and lower limits. The shaded band shows the allowed region and the horizontal bisector of the central value of $\mathcal{BR}(B^0 \to \bar{D}^0 f_0(500)) = (11.2 \pm 2.4) \times 10^{-5}$ for data.

of the σ meson. The authors of Ref. [21] assumed that σ has the similar decay constant and LCDAs as those of $f_0(980)$, while the authors of Ref. [23] just took the same decay constant and LCDAs with those of $a_0(980)$. These two sets of parameters will generate very different results: If using the former, one will obtain small branching ratios which are far below the experimental lower limit in all the mixing angle region, but the predicted branching ratio will overlap with the data in some angle values by using the latter, which can be found in Fig. 4. It shows that the decay constant and LCDAs of σ is closer to those of $a_0(980)$, so they should have the similar quark components and structure. From Fig. 4, we find that there also exist two allowed mixing angle regions 28°–64° and 116°–152°, where the former region can overlap mostly with the allowed region 22°–58° obtained from the analysis of $B^0 \to \bar{D}^0 f_0(980)$ and $B_s \to \bar{D}^0 f_0(980)$ decays. While the two large angle regions have less coincidence, it seems that the small angle region is more favored than the large one.

In order to predict other $B_{(s)}$ charmed decays, the mixing angle is taken as two values 34° and 38° (certainly, one can get similar branching ratios by taking $\theta = 142°$ and 154°, if they cannot be excluded by the future data), one of which is consistent with $\theta = 30° \pm 3°$ obtained by averaging over several processes [5]. Then the branching ratios of these CKM suppressed decays $B^0 \to D^0 f_0(980)$, $B_s \to D^0 f_0(980)$, $B^+ \to D^+ f_0(980)$, and $B^+ \to D_s^+ f_0(980)$ are listed in Table I. The pseudoscalar meson $D_{(s)}$ is replaced by the vector meson $D_{(s)}^*$ in our considering decays, and the branching ratios of the corresponding channels are listed in Table II. From our calculations, we find that the branching ratios of the B_s decays are not very sensitive to the mixing angle θ; especially for $\mathcal{BR}(B_s \to D^0 f_0)$, its value changes in the range of

TABLE I. The CP-averaged branching ratios ($\times 10^{-6}$) of $B \to Df_0(980)$ obtained by taking the mixing angle $\theta = 34°$ and 38°, respectively. The first uncertainty comes from the $\omega_b = 0.4 \pm 0.1(0.5 \pm 0.1)$ for $B(B_s)$ mesons, the second and the third uncertainties are from the decay constant $\bar{f}_{f_0} = 0.18 \pm 0.015$ GeV and the Gegenbauer moment $B_1 = -0.78 \pm 0.08$ of the $f_0(980)$ meson, respectively, and the last one comes from $C_{D_{(s)}} = 0.5(0.4) \pm 0.1$ for the $D_{(s)}$ meson.

	34°	38°
$\mathcal{BR}(B \to D^0 f_0)[\times 10^{-9}]$	$4.45^{+2.25+0.96+0.71+0.35}_{-1.42-0.85-0.63-0.33}$	$5.39^{+2.72+1.16+0.86+0.43}_{-1.71-1.04-0.77-0.41}$
$\mathcal{BR}(B_s \to D^0 f_0)[\times 10^{-7}]$	$1.32^{+1.02+0.30+0.21+0.19}_{-0.60-0.27-0.20-0.17}$	$1.29^{+0.99+0.29+0.21+0.18}_{-0.55-0.27-0.19-0.16}$
$\mathcal{BR}(B^+ \to D^+ f_0)[\times 10^{-7}]$	$1.00^{+0.37+0.16+0.06+0.01}_{-0.26-0.15-0.06-0.01}$	$1.22^{+0.45+0.19+0.08+0.01}_{-0.32-0.18-0.08-0.01}$
$\mathcal{BR}(B^+ \to D_s^+ f_0)[\times 10^{-6}]$	$2.30^{+0.96+0.32+0.11+0.07}_{-0.67-0.30-0.11-0.06}$	$2.97^{+1.20+0.43+0.16+0.07}_{-0.83-0.40-0.15-0.07}$

TABLE II. Same as Table I except for the decays $B \to \bar{D}^*(D^*)f_0(980)$.

	34°	38°
$\mathcal{BR}(B \to \bar{D}^{*0} f_0)[\times 10^{-6}]$	$7.40^{+2.33+1.32+2.32+0.75}_{-1.84-1.26-1.78-0.73}$	$8.97^{+2.83+1.60+2.82+0.91}_{-2.23-1.52-2.16-0.89}$
$\mathcal{BR}(B_s \to \bar{D}^{*0} f_0)[\times 10^{-6}]$	$1.63^{+0.72+0.31+0.48+0.20}_{-0.50-0.29-0.38-0.17}$	$1.43^{+0.62+0.27+0.42+0.17}_{-0.44-0.25-0.33-0.15}$
$\mathcal{BR}(B \to D^{*0} f_0)[\times 10^{-9}]$	$6.48^{+3.57+1.37+0.64+0.33}_{-2.24-1.23-0.56-0.31}$	$7.86^{+4.33+1.66+0.78+0.40}_{-2.72-1.49-0.68-0.37}$
$\mathcal{BR}(B_s \to D^{*0} f_0)[\times 10^{-7}]$	$2.06^{+1.79+0.46+0.20+0.20}_{-0.98-0.41-0.18-0.17}$	$1.94^{+1.63+0.44+0.19+0.19}_{-0.90-0.39-0.17-0.16}$
$\mathcal{BR}(B^+ \to D^{*+} f_0)[\times 10^{-7}]$	$2.07^{+0.69+0.38+0.16+0.02}_{-0.49-0.34-0.15-0.02}$	$2.51^{+0.84+0.46+0.19+0.02}_{-0.60-0.42-0.19-0.03}$
$\mathcal{BR}(B^+ \to D_s^{*+} f_0)[\times 10^{-6}]$	$5.00^{+1.68+0.94+0.37+0.07}_{-1.21-0.88-0.39-0.06}$	$6.10^{+2.04+1.14+0.45+0.08}_{-1.47-1.06-0.47-0.10}$

$(1.2\text{–}1.8) \times 10^{-7}$ when the mixing angle varies from 0° to 180°. The reason is as follows: The amplitude from the $s\bar{s}$ component has a large imaginary part and a small real part. It is contrary for the amplitude from the $q\bar{q} = (u\bar{u} + d\bar{d})/\sqrt{2}$ component, where the real part is about one order larger than the imaginary part. When the real and imaginary parts from the $s\bar{s}$ and $q\bar{q} = (u\bar{u} + d\bar{d})/\sqrt{2}$ amplitudes are mixed through Eq. (1), respectively, the former (latter) is dominated by the sine (cosine) law, but the later is stronger than the former, so these two kinds of contrary change trends make the total amplitude changes in a much milder cosine curve. The branching ratios of all the B decay modes are dependent on the mixing angle via $\sin\theta$ (maybe with an initial phase), just like the left panel in Fig. 2, while those of the B_s decay modes are dependent on the mixing angle via $\cos\theta$ with an initial phase, just like the right panel in Fig. 2.

V. CONCLUSION

In this paper, first we analyze the decays $B \to \bar{D}^0 f_0(980)$ and $B_s \to \bar{D}^0 f_0(980)$ carefully in the pQCD factorization approach and find two possible regions for the mixing angle θ; one is centered at 34°–38° and the other is near 142°–154°. If the data of the decay $B^0 \to \bar{D}^0 \sigma$ are also included, we find that the small angle region is more favored. Our analyses support that the two-quark component in $f_0(980)$ is dominant in the B decay dynamic mechanism, and the $s\bar{s}$ component is more important than the $q\bar{q}$ component. Certainly other components, such as gluon, the four-quark component, and the $K\bar{K}$ threshold effect, may also give some influences. It is noticed that our picture is not in conflict with the popular explanation of the dominant four-quark component in $f_0(980)$. Then we predict the branching ratios of other $B_{(s)} \to D_{(s)} f_0(980)$, $D^*_{(s)} f_0(980)$ decay channels by fixing $\theta = 34°$ and 38°, respectively, and we find that the branching ratios of B_s decay modes are less sensitive to the mixing angle compared with those of B decay modes. Especially, for the decay $B_s \to D^0 f_0$, its branching ratio changes in a small region between $(1.2\text{–}1.8) \times 10^{-7}$ with the mixing angle θ running from 0° to 180°.

ACKNOWLEDGMENTS

This work is partly supported by the National Natural Science Foundation of China under Grant No. 11347030, by the Program of Science and Technology Innovation Talents in Universities of Henan Province 14HASTIT037. Z. Q. Z. is grateful to Hai-Yang Cheng and Hsiang-nan Li for carefully reading the manuscript and very useful suggestions, and to Wen-Fei Wang, Henry T. Wong, and Tzu-Chiang Yuan for helpful discussions. He also thanks the Institute of Physics, Academia Sinica for their hospitalities during his visit when part of this work was done.

APPENDIX A: DECAY AMPLITUDES

For the CKM suppressed decays, for example, $B \to D^0 f_0(980)$, their Feynman diagrams to leading order will be different from Fig. 1, especially for the (non)factorizable annihilation diagrams, where the positions of D and $f_0(980)$ are exchanged compared with those of the $B \to \bar{D}^0 f_0(980)$ decay. But the factorizable emission diagrams are the same with each other, so $\mathcal{F}^D_{B\to f_0} = \mathcal{F}^{\bar{D}}_{B\to f_0}$. Here we also list other amplitudes of these CKM suppressed decays,

$$\begin{aligned}\mathcal{M}^D_{B\to f_0} = {} & 32\pi C_f m_B^4/\sqrt{2N_C}\int_0^1 dx_1dx_2dx_3\int_0^\infty b_1db_1b_3db_3\phi_B(x_1,b_1)\phi_D(x_3,b_3)\\ & \times\{[(x_3-x_1)\phi_{f_0}(x_2)-r_{f_0}x_2(\phi^s_{f_0}(x_2)-\phi^t_{f_0}(x_2))]\\ & \times E_{en}(t_d)h^d_{en}(x_1,x_2(1-r_D^2),x_3,b_1,b_3)+E_{en}(t_c)h^c_{en}(x_1,x_2(1-r_D^2),x_2,b_1,b_3)\\ & \times[(x_1-x_2+x_3-1)\phi_{f_0}(x_2)+r_{f_0}x_2(\phi^s_{f_0}(x_2)+\phi^t_{f_0}(x_2))]\},\end{aligned} \tag{A1}$$

$$\begin{aligned}\mathcal{M}^{f_0}_{ann} = {} & 32\pi C_f m_B^4/\sqrt{2N_C}\int_0^1 dx_1dx_2dx_3\int_0^\infty b_1db_1b_3db_3\phi_B(x_1,b_1)\phi_D(x_3,b_3)\\ & \times\{E_{an}(t_e)h^e_{an}(x_1,x_2,x_3,b_1,b_3)[(1-r_b-x_2)\phi_{f_0}(x_2)+r_Dr_{f_0}((2-4r_b-x_2-x_3)\phi^s_{f_0}(x_2)-(x_2-x_3)\phi^t_{f_0}(x_2))]\\ & +E_{an}(t_f)h^f_{an}(x_1,x_2,x_3,b_1,b_2)[x_3\phi_{f_0}(x_2)+r_Dr_{f_0}((x_2+x_3)\phi^s_{f_0}(x_2)+(x_3-x_2)\phi^t_{f_0}(x_2))]\},\end{aligned} \tag{A2}$$

$$\begin{aligned}\mathcal{F}^{f_0}_{ann} = {} & 8\pi C_f f_B m_B^4\int_0^1 dx_2dx_3\int_0^\infty b_2db_2b_2db_2\phi_D(x_3,b_3)\{[(r_D^2-1)x_3\phi_{f_0}(x_2)\\ & -2r_{f_0}r_D(1-r_D^2+x_3)\phi^s_{f_0}(x_2)]E_{af}(t'_g)h_{af}(x_3,(1-x_2)(1-r_D^2),b_3,b_2)\\ & +E_{af}(t'_h)h_{af}(x_2,x_3(1-r_D^2),b_2,b_3)[(x_2-2r_Dr_c)\phi_{f_0}(x_2)+2r_Dr_{f_0}((x_2+1)\phi^s_{f_0}(x_2)+(x_2-1)\phi^t_{f_0}(x_2))]\}.\end{aligned} \tag{A3}$$

Here we do not show the amplitudes of the decays $B_{(s)} \to \bar{D}^*(D^*)f_0(980)$, because one can obtain them from those of the decays $B_{(s)} \to \bar{D}(D)f_0(980)$ by the substitutions $m_D \to m_{D^*}$, $f_D \to f_{D^*}$, $\phi_D \to \phi_{D^*}$, where the terms including r_D^2, $r_Dr_{f_0}$, and r_Dr_c were neglected. It is similar for the decays involving the D_s^* meson.

APPENDIX B: HARD SCALES

$$t_a = \max\left(\sqrt{x_2(1-r_D^2)}m_B, 1/b_1, 1/b_2\right), \tag{B1}$$

$$t_b = \max\left(\sqrt{x_1(1-r_D^2)}m_B, 1/b_1, 1/b_2\right), \tag{B2}$$

$$t_{c,d} = \max\left(\sqrt{x_1x_2(1-r_D^2)}m_B, \sqrt{|A^2_{c,d}|}m_B, 1/b_1, 1/b_3\right), \tag{B3}$$

$$t_{e,f} = \max\left(\sqrt{x_2x_3(1-r_D^2)}m_B, \sqrt{|L^2_{e,f}|}, m_B, 1/b_1, 1/b_3\right), \tag{B4}$$

$$t_g = \max\left(\sqrt{(1-x_2)(1-r_D^2)}m_B, 1/b_2, 1/b_3\right), \tag{B5}$$

$$t_h = t'_g = \max\left(\sqrt{x_3(1-r_D^2)}m_B, 1/b_2, 1/b_3\right), \tag{B6}$$

$$t'_h = \max\left(\sqrt{x_2(1-r_D^2)}m_B, 1/b_2, 1/b_3\right). \tag{B7}$$

And the $S_j(t)(j = B, D, f_0)$ functions in Sudakov form factors in Eqs. (20), (21), (29), and (30) are listed as

$$S_B(t) = s\left(x_1\frac{m_B}{\sqrt{2}}, b_1\right) + 2\int_{1/b_1}^t \frac{d\bar{\mu}}{\bar{\mu}}\gamma_q(\alpha_s(\bar{\mu})), \tag{B8}$$

$$S_D(t) = s\left(x_3\frac{m_B}{\sqrt{2}}, b_3\right) + 2\int_{1/b_3}^t \frac{d\bar{\mu}}{\bar{\mu}}\gamma_q(\alpha_s(\bar{\mu})), \tag{B9}$$

$$\begin{aligned}S_{f_0}(t) = {} & s\left(x_2\frac{m_B}{\sqrt{2}}, b_2\right) + s\left((1-x_2)\frac{m_B}{\sqrt{2}}, b_2\right)\\ & + 2\int_{1/b_2}^t \frac{d\bar{\mu}}{\bar{\mu}}\gamma_q(\alpha_s(\bar{\mu})),\end{aligned} \tag{B10}$$

where the quark anomalous dimension is $\gamma_q = -\alpha_s/\pi$, and the expression of the $s(Q, b)$ in the one-loop running coupling constant is used,

$$s(Q,b)=\frac{A^{(1)}}{2\beta_1}\hat{q}\ln\left(\frac{\hat{q}}{\hat{b}}\right)-\frac{A^{(1)}}{2\beta_1}(\hat{q}-\hat{b})+\frac{A^{(2)}}{4\beta_1^2}\left(\frac{\hat{q}}{\hat{b}}-1\right)-\left[\frac{A^{(2)}}{4\beta_1^2}-\frac{A^{(1)}}{4\beta_1}\ln\left(\frac{e^{2\gamma_E-1}}{2}\right)\right]\ln\left(\frac{\hat{q}}{\hat{b}}\right), \tag{B11}$$

where the variables are defined by $\hat{q}=\ln[Q/(\sqrt{2}\Lambda)]$, $\hat{q}=\ln[1/(b\Lambda)]$ and the coefficients $A^{(1,2)}$ and β_1 are

$$\beta_1=\frac{33-2n_f}{12},\qquad A^{(1)}=\frac{4}{3}, \tag{B12}$$

$$A^{(2)}=\frac{67}{9}-\frac{\pi^2}{3}-\frac{10}{27}n_f+\frac{8}{3}\beta_1\ln\left(\frac{1}{2}e^{\gamma_E}\right), \tag{B13}$$

where n_f is the number of the quark flavors and γ_E the Euler constant.

[1] R. L. Jaffe, Phys. Rev. D **15**, 267 (1977); **15**, 281 (1977).
[2] P. Minkowski and W. Ochs, Eur. Phys. J. C **9**, 283 (1999).
[3] A. Gokalp, Y. Sarac, and O. Yilmaz, Phys. Lett. B **609**, 291 (2005).
[4] J. W. Li, D. S. Du, and C. D. Lu, Eur. Phys. J. C **72**, 2229 (2012).
[5] W. Ochs, J. Phys. G **40**, 043001 (2013).
[6] S. Stone and L. Zhang, Phys. Rev. Lett. **111**, 062001 (2013).
[7] T. Feldmann, P. Kroll, and B. Stech, Phys. Rev. D **58**, 114006 (1998).
[8] T. Feldmann, P. Kroll, and B. Stech, Phys. Lett. B **449**, 339 (1999).
[9] Y. D. Tsai, H. n. Li, and Q. Zhao, Phys. Rev. D **85**, 034002 (2012).
[10] R. Aaij *et al.* (LHCb Collaboration), Phys. Rev. D **92**, 032002 (2015).
[11] R. Aaij *et al.* (LHCb Collaboration), J. High Energy Phys. 08 (2015) 005.
[12] R. H. Li, C. D. Lu, and H. Zou, Phys. Rev. D **79**, 014013 (2009).
[13] H. Zou, R. H. Li, X. X. Wang, and C. D. Lu, J. Phys. G **37**, 015002 (2010).
[14] Z. Q. Zhang, J. Phys. G **36**, 125004 (2009).
[15] Z. Q. Zhang, Phys. Rev. D **87**, 074030 (2013).
[16] C. S. Kim, R. H. Li, and W. Wang, Phys. Rev. D **88**, 034003 (2013).
[17] C. D. Lu and M. Z. Yang, Eur. Phys. J. C **28**, 515 (2003).
[18] T. Kurimoto, H.-n. Li, and A. I. Sanda, Phys. Rev. D **67**, 054028 (2003).
[19] K. A. Olive *et al.* (Particle Data Group Collaboration), Chin. Phys. C **38**, 090001 (2014).
[20] D. Becirevic, Ph. Boucaud, J. P. Leroy, V. Lubicz, G. Martinelli, F. Mescia, and F. Rapuano, Phys. Rev. D **60**, 074501 (1999); M. A. Ivanov, J. G. Korner, and P. Santorelli, Phys. Rev. D **73**, 054024 (2006); G. L. Wang, Phys. Lett. B **633**, 492 (2006).
[21] H. Y. Cheng and K. C. Yang, Phys. Rev. D **73**, 014017 (2006).
[22] F. De Fazio and M. R. Pennington, Phys. Lett. B **521**, 15 (2001).
[23] R. H. Li, C. D. Lu, W. Wang, and X. X. Wang, Phys. Rev. D **79**, 014013 (2009).